1 Introduction to Block Copolymers

I. W. HAMLEY
Department of Chemistry, University of Leeds, Leeds LS2 9JT, UK

1.1 INTRODUCTION

Block copolymers are useful in many applications where a number of different polymers are connected together to yield a material with hybrid properties. For example, thermoplastic elastomers are block copolymers containing a rubbery matrix (polybutadiene or polyisoprene) containing glassy hard domains (often polystyrene). The block copolymer, a kind of polymer alloy, behaves as a rubber at ambient conditions, but can be moulded at high temperatures due to the presence of the glassy domains that act as physical crosslinks. In solution, attachment of a water soluble polymer to an insoluble polymer leads to the formation of micelles in amphiphilic block copolymers. The presence of micelles leads to structural and flow characteristics of the polymer in solution that differ from either parent polymer.

A block copolymer molecule contains two or more polymer chains attached at their ends. Linear block copolymers comprise two or more polymer chains in sequence, whereas a starblock copolymer comprises more than two linear block copolymers attached at a common branch point. Polymers containing at least three homopolymers attached at a common branching point have been termed mixed arm block copolymers, although they can also be viewed as multigraft copolymers.

In the following, block copolymers prepared by controlled polymerization methods only are considered, primarily di- and tri-block copolymers (see Figure 1.1). Multiblock copolymers such as polyurethanes and poly (urethane-ureas) prepared by condensation polymerisation are not discussed. Whilst these materials do exhibit microphase separation, it is only short range in spatial extent due to the high polydispersity of the polymers.

A standard notation for block copolymers is becoming accepted, whereby X-*b*-Y denotes a diblock copolymer of polymer X and polymer Y. However, sometimes the *b* is replaced by the full term *block*, or alternatively is omitted, and the diblock is denoted X-Y.

A number of texts covering general aspects of block copolymer science and engineering appeared in the 1970s and 1980s and these are listed elsewhere [1]. More recently, specialised reviews have appeared on block copolymer melts and

Developments in Block Copolymer Science and Technology. Edited by I. W. Hamley
 ISBN: 0–470–84335–7

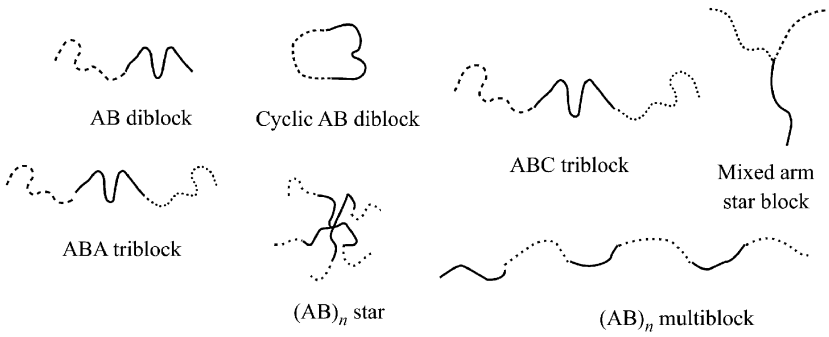

Figure 1.1 Block copolymer architectures.

block copolymer solutions, and these are cited in Sections 1.3 and 1.4 below. The burgeoning interest in block copolymers is illustrated by contributions covering various aspects of the subject in a review journal [2] and in a book [3].

Since the excellent review by Riess *et al*. [4] there have been many advances in the field of block copolymer science and engineering, including new synthesis methods, developments in the understanding of phase behaviour and the investigation of structure and dynamics in thin films. Many of these advances are likely to lead soon to novel applications.

1.2 SYNTHESIS

The main techniques for synthesis of block copolymers in research labs around the world are presently anionic polymerization and controlled radical polymerization methods. The older technique of anionic polymerization is still used widely in the industrial manufacture of block copolymers. Cationic polymerization may be used to polymerize monomers that cannot be polymerized anionically, although it is used for only a limited range of monomers. A summary of block copolymer synthesis techniques has been provided by Hillmyer [5].

1.2.1 ANIONIC POLYMERIZATION

Anionic polymerization is a well-established method for the synthesis of tailored block copolymers. The first anionic polymerizations of block copolymers were conducted as early as 1956 [6]. To prepare well-defined polymers, the technique is demanding, requiring high-purity starting reagents and the use of high-vacuum procedures to prevent accidental termination due to the presence of impurities. In the lab, it is possible to achieve polydispersities $M_w/M_n < 1.05$ via anionic polymerization. The method is also used industrially to prepare

several important classes of block copolymers including SBS-type thermoplastic elastomers (S = polystyrene, B = polybutadiene) and polyoxyethylene-*b*-polyoxypropylene-*b*-polyoxyethylene Pluronic amphiphilic copolymers [3]. The principles of anionic polymerization are discussed in Chapter 2. There are a number of reviews that cover its application to block copolymers [7–11]. Recent advances have mainly been directed towards the synthesis of block copolymers with exotic architectures, such as mixed arm stars [12–14], H-shaped copolymers [12], ring-shaped (cyclic) block copolymers [15], etc. All of these require the careful choice of multifunctional initiators.

1.2.2 LIVING RADICAL POLYMERIZATION

Undoubtedly the main advance in block copolymer synthesis in the last decade has been the development of techniques of living radical polymerization (sometimes termed controlled radical polymerization). The principle of controlled radical polymerization methods is to establish a dynamic equilibrium between a small fraction of growing free radicals and a large majority of dormant species. Generated free radicals propagate and terminate as in conventional radical polymerization, although the presence of only a small fraction of radicals prevents premature termination. Among living polymerization methods, atom-transfer radical polymerization (ATRP) has been used most extensively to synthesize block copolymers. Here, the radicals are generated through a reversible redox process catalysed by a transition metal complex that undergoes a one-electron oxidation with the abstraction of a halogen atom from the dormant species. The ATRP method, and its application to the synthesis of block copolymers, has recently been reviewed [16].

ATRP has been used to prepare AB diblock, ABA triblock and most recently ABC triblock copolymers [17]. To date, the technique has been used to create block copolymers based on polystyrene and various polyacrylates [16]. However, it is possible to synthesize a so-called macroinitiator by other polymerization mechanisms (anionic, cationic, etc.), and use this in the ATRP of vinyl monomers. Examples, such as the anionic polymerization of PEO macroinitiators for ATRP synthesis of PEO/PS block copolymers, are discussed by Matyjaszewski and Xia [16].

1.2.3 OTHER METHODS

Sequential living cationic polymerization is primarily used to prepare block copolymers containing a vinyl ether block, or polyisobutylene [18–20]. It can also be coupled with other techniques [18,20]. However, the range of monomers that may be polymerized by this method is comparatively limited and consequently living cationic polymerization is only used in prescribed circumstances.

Ring-opening metathesis polymerization has also been exploited to build blocks from cyclic olefins, especially polynorbornene [5]. The development of ROMP for block copolymer synthesis has recently been facilitated by the introduction of functional-group-tolerant metathesis catalysts by Grubbs [21].

1.3 BLOCK COPOLYMER MELTS

The interest in the phase behaviour of block copolymer melts stems from microphase separation of polymers that leads to nanoscale-ordered morphologies. This subject has been reviewed extensively [1,22–24]. The identification of the structure of bicontinuous phases has only recently been confirmed, and this together with major advances in the theoretical understanding of block copolymers, means that the most up-to-date reviews should be consulted [1,24]. The dynamics of block copolymer melts, in particular rheological behaviour and studies of chain diffusion via light scattering and NMR techniques have also been the focus of several reviews [1,25,26].

The phase behaviour of block copolymer melts is, to a first approximation, represented in a morphology diagram in terms of χN and f [1]. Here f is the volume fraction of one block and χ is the Flory–Huggins interaction parameter, which is inversely proportional to temperature, which reflects the interaction energy between different segments. The configurational entropy contribution to the Gibbs energy is proportional to N, the degree of polymerization. When the product χN exceeds a critical value, $(\chi N)_{\mathrm{ODT}}$ (ODT = order–disorder transition) the block copolymer microphase separates into a periodically ordered structure, with a lengthscale $\sim 5 - 500\,\mathrm{nm}$. The structure that is formed depends on the copolymer architecture and composition [1]. For diblock copolymers, a lamellar (lam) phase is observed for symmetric diblocks ($f = 0.5$), whereas more asymmetric diblocks form hexagonal-packed cylinder (hex) or body-centred cubic (bcc) spherical structures. A complex bicontinuous cubic gyroid (gyr) (spacegroup $Ia\bar{3}d$) phase has also been identified [27,28] for block copolymers between the lam and hex phases near the ODT, and a hexagonal-perforated layer (hpl) phase has been found to be metastable in this region [29–31]. A useful compilation is available of studies on the morphology of block copolymers of various chemistries [32].

The main techniques for investigating solid block copolymer microstructures are transmission electron microscopy (TEM) and small-angle X-ray or neutron scattering. TEM provides direct images of the structure, albeit over a small area of the sample. Usually samples are stained using the vapours from a solution of a heavy metal acid (OsO_4 or RuO_4) to increase the contrast for electrons between domains [33]. Small-angle scattering probes the structure over the whole sample volume, giving a diffraction pattern. The positions of the reflections in the diffraction pattern can be indexed to identify the symmetry of the phase [1,22]. The preparation method can have a dramatic influence

on the apparent morphology, for example whether solvent casting or melt processing is performed. Numerous cases of mistaken identification of "equilibrium phases" have appeared in the literature, when the phase was simply an artifact. For instance, Lipic *et al.* [34] obtained different morphologies by varying the preparation conditions for a polyolefin diblock examined by them. In other cases, phases such as hexagonal perforated layers have been observed [29], which, although reproducible, have turned out to be only long-lived metastable phases, ultimately transforming to the equilibrium gyroid phase [30,31]. The ODT in block copolymers can be located via a number of methods – from discontinuities in the dynamic shear modulus [35–37] or small-angle scattering peak shape [38,39] or from calorimetry measurements [40].

To establish relationships between different block copolymer phase diagrams and also to facilitate comparison with theory, it is necessary to specify parameters in addition to χN and f. First, asymmetry of the conformation of the copolymer breaks the symmetry of the phase diagram about $f = 0.5$. For AB diblocks, conformational asymmetry is quantified using the "asymmetry parameter" $\varepsilon = (b_A^2/v_A)/(b_B^2/v_B)$ [41,42], where b_J is the segment length for block J and v_J is the segment volume. Composition fluctuations also modify the phase diagram, and this has been accounted for theoretically via the Ginzburg parameter $\bar{N} = Nb^6\rho^2$, where ρ is the number density of chains [43,44]. The extent of segregation of block copolymers depends on the magnitude of χN. For small χN, close to the order–disorder transition (up to $\chi N = 12$ for symmetric diblocks for which $\chi N_{\mathrm{ODT}} = 10.495$), the composition profile (density of either component) is approximately sinusoidal. This is termed the weak-segregation limit. At much larger values of $\chi N (\chi N >\sim 100)$, the components are strongly segregated and each domain is almost pure, with a narrow interphase between them. This is the strong-segregation limit.

The first theories for block copolymers were introduced for the strong-segregation limit (SSL) and the essential physical principles underlying phase behaviour in the SSL were established in the early 1970s [1]. Most notably, Helfand and coworkers [45–47] developed the self-consistent field (SCF) theory, this permitting the calculation of free energies, composition profiles and chain conformations. In the SCF theory, the external mean fields acting on a polymer chain are calculated self-consistently with the composition profile. The theory of Leibler [48] describes block copolymers in the weak-segregation limit. It employs a Landau–Ginzburg approach to analyse the free energy, which is expanded with reference to the average composition profile. The free-energy coefficients are computed within the random-phase approximation. Weak-segregation limit theory can be extended to allow for thermal-composition fluctuations. This changes the mean-field prediction of a second-order phase transition for a symmetric diblock copolymer to a first-order transition. Fredrickson and Helfand [43] studied this effect for block copolymers and showed that composition fluctuations, incorporated via the renormalization method of Brazovskii,

lead to a "finite-size effect", where the phase diagram depends on $\bar{N}$. A powerful new method to solve the self-consistent field equations for block copolymers has been applied by Matsen and coworkers [49–52] to analyse the ordering of many types of block copolymer in bulk and in thin films. The strong- and weak-segregation limits are spanned, as well as the intermediate regime where the other methods do not apply. This implementation of SCF theory predicts phase diagrams, and other quantities such as domain spacings, in good agreement with experiment (see Figure 1.2) and represents an impressive state-of-the-art for modelling the ordering of soft materials. Accurate liquid-state theories have also been used to model block copolymer melts [53,54], although

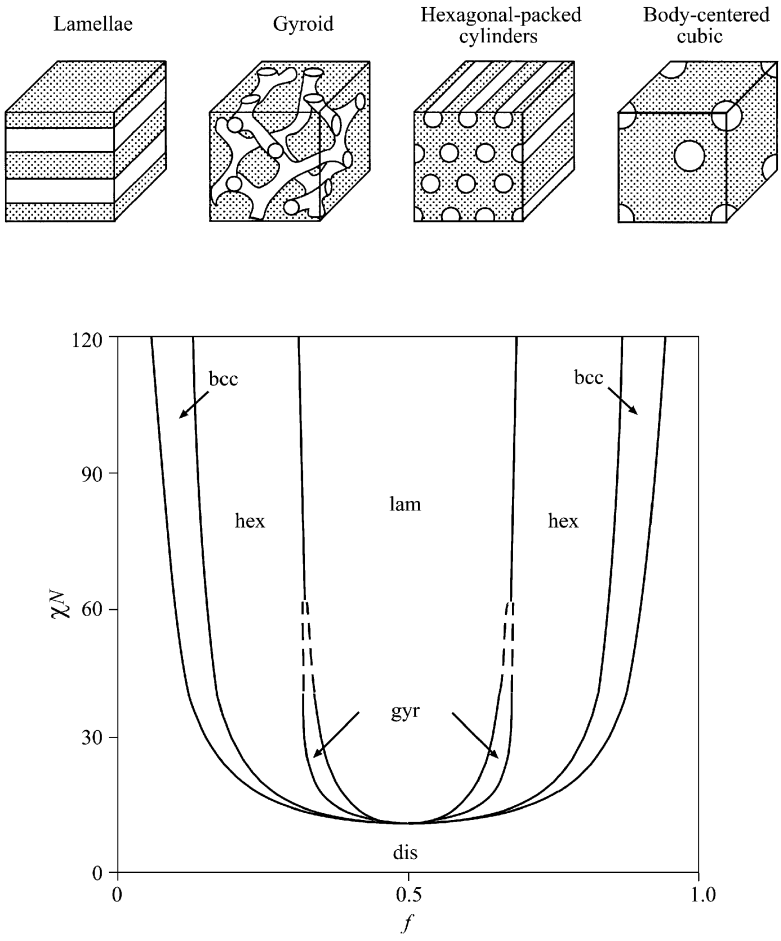

Figure 1.2 Phase diagram for a conformationally symmetric diblock copolymer, calculated using self-consistent mean field theory [49, 51], along with illustrations of the equilibrium morphologies. In the phase diagram, regions of stability of disordered (dis), lamellar (lam), gyroid (gyr), hexagonal (hex) and body-centred cubic (bcc) phases are indicated.

they are hard to implement and consequently the method is often, regrettably, overlooked [1]. Recently, a method has been developed to directly simulate field theories for polymers without introducing approximations such as mean-field approaches, perturbation expansions, etc. [55]. This technique holds much promise for examining the thermodynamics of block copolymers in the limit of low molecular weight where approximate methods such as mean-field theory or renormalization techniques break down.

A phase diagram computed using self-consistent mean field theory [49,51] is shown in Figure 1.2. This shows the generic sequence of phases accessed just below the order–disorder transition temperature for diblock copolymers of different compositions. The features of phase diagrams for particular systems are different in detail, but qualitatively they are similar, and well accounted for by SCF theory.

The phase behaviour of ABC triblocks is much richer [24] than two-component diblocks or triblocks, as expected because multiple interaction parameters (χ_{AB}, χ_{AC} and χ_{BC}) result from the presence of a distinct third block. Summaries of work on ABC triblock morphologies have appeared [1,56]. Because of the large number of possible morphologies, theorists are presently working to predict the phase behaviour of these copolymers using methods that do not require *a priori* knowledge of the space group symmetries of trial structures [57,58].

During processing, block copolymers are subjected to flow. For example, thermoplastic elastomers formed by polystyrene-*b*-polybutadiene-*b*-polystyrene (SBS) triblock copolymers, are moulded by extrusion. This leads to alignment of microphase-separated structures. This was investigated in the early 1970s by Keller and co-workers [22,59] who obtained transmission electron micrographs from highly oriented specimens of Kraton SBS copolymers following extrusion. Examples are included in Figure 1.3. Work on the effect of flow on block copolymer melts has been reviewed [1,25,60,61]. Due to the convenience and well-defined nature of the shear geometry, most model studies have exploited this type of flow. The application of shear leads to orientation of block copolymer microstructures at sufficiently high shear rates and/or strain amplitudes (in the case of oscillatory shear). Depending on shear conditions and temperature, different orientations of a morphology with respect to the shear plane can be accessed. This has been particularly well studied for the lamellar phase where so-called "parallel" (lamellar normal along shear gradient direction) and "perpendicular" (lamellar normal along the neutral direction) orientations have been observed [62]. Distinct orientation states of hexagonal and cubic phases have also been investigated, details being provided elsewhere [61]. The ability to generate distinct macroscopic orientation states of block copolymers by shear is important in future applications of block copolymers, where alignment will be important (reinforced composites, optoelectronic materials and separation media). Shear also influences thermodynamics, since the order–disorder transition shifts upwards on increasing shear rate because the ordered phase is stabilized under shear [63,64].

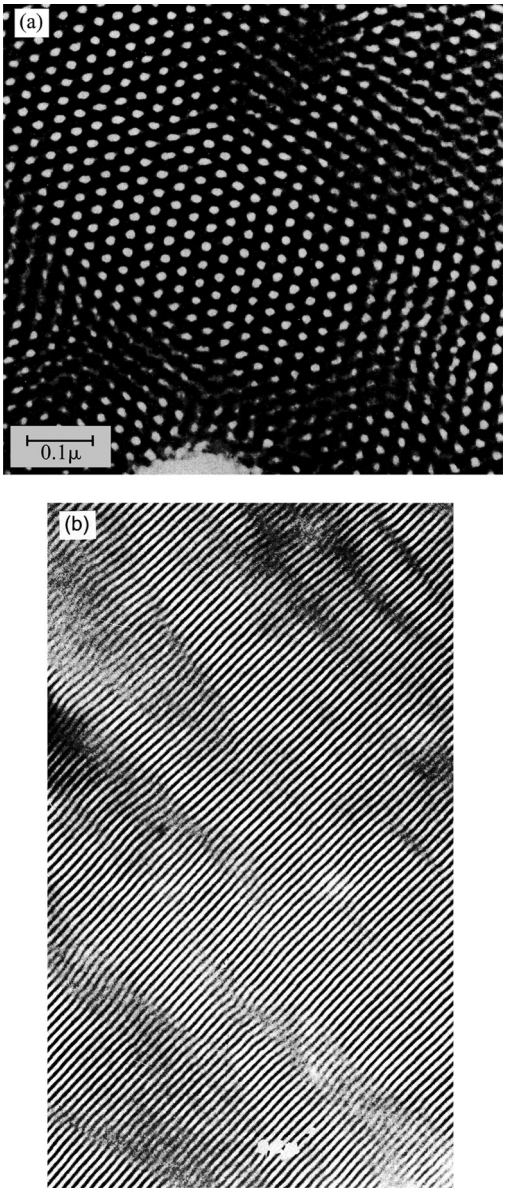

Figure 1.3 TEM micrographs from a hexagonal-packed cylinder structure subjected to flow during high-temperature extrusion. The sample was a PS-PB-PS tribock (Kraton D1102 [209]). (a) Perpendicular to the extrusion direction, (b) a parallel section.

The phase behaviour of rod–coil block copolymers is already known to be much richer than that of coil–coil block copolymers, because the rod block can orient into liquid-crystal structures [1]. The rod block may be analogous to a biomacromolecule, for example poly(benzyl glutamates) [65,66] and polypeptides [67] forming helical rod-like blocks have been incorporated in block copolymers. Possible applications of these materials arising from their biocompatibility are evident.

1.4 BLOCK COPOLYMER FILMS

Microphase separation by block copolymers in thin films has been investigated from several perspectives. First, the physics of self-assembly in confined soft materials can be studied using model block copolymer materials for which reliable mean-field statistical mechanical theories have been developed [68]. Second, interest has expanded due to potential exciting applications that exploit self-organization to fabricate high-density data-storage media [69], to lithographically pattern semiconductors with ultrasmall feature sizes [70,71] or to prepare ultrafine filters or membranes [72]. Research in this field is growing at a rapid pace, and the field has not been reviewed since 1998 [1,73], since when many new developments have occurred.

Block copolymer films can be prepared by the spin-coating technique, where drops of a solution of the polymer in a volatile organic solvent are deposited on a spinning solid substrate (often silicon wafers are used due to their uniform flatness). The polymer film spreads by centrifugal forces, and the volatile solvent is rapidly driven off. With care, the method can give films with a low surface roughness over areas of square millimetres. The film thickness can be controlled through the spin speed, the concentration of the block copolymer solution or the volatility of the solvent, which also influences the surface roughness [74]. Dip coating is another reliable method for fabricating uniform thin films [75]. Whatever the deposition technique, if the surface energy of the block copolymer is much greater than that of the substrate, dewetting will occur. The mechanism of dewetting has been investigated [76–78].

In thin films, the lamellae formed by symmetric block copolymers can orient either parallel or perpendicular to the substrate. A number of possible arrangements of the lamellae are possible, depending on the surface energies of the blocks and that of the substrate, and whether the film is confined at one or both surfaces. These are illustrated in Figure 1.4. In the case that a different block preferentially wets the interface with the substrate or air, wetting is asymmetric and a uniform film has a thickness $(n+\frac{1}{2})d$. If the initial film thickness is not equal to $(n+\frac{1}{2})d$, then islands or holes (quantized steps of height d) form to conserve volume [79]. As well as leading to distinct orientations, confinement of block copolymers can change the thermodynamics of ordering, in particular surface-induced ordering persists above the bulk order–disorder transition [80].

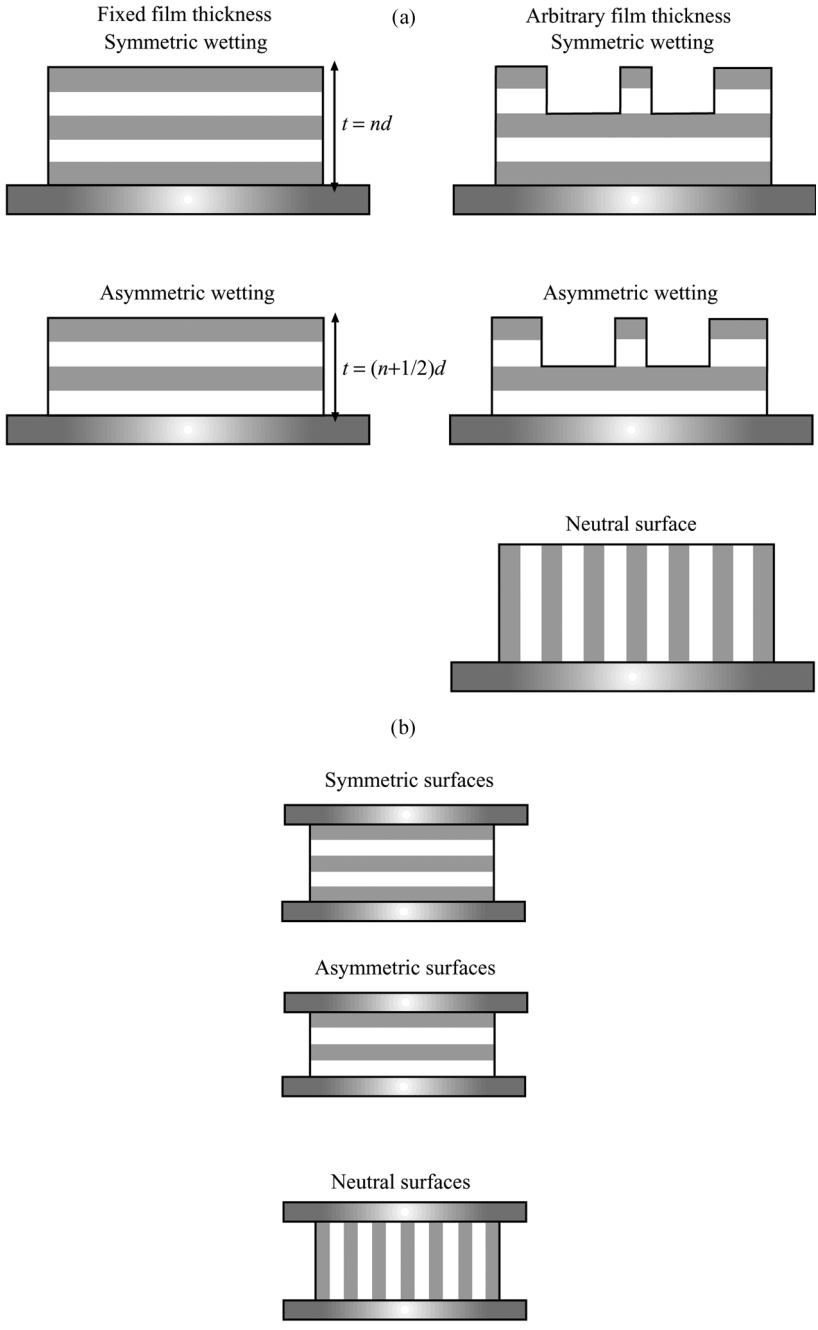

Figure 1.4 Possible configurations of lamellae in block copolymer films. (a) Confined at one surface. (b) Confined at both surfaces.

Asymmetric block copolymers that form hexagonal or cubic-packed spherical morphologies in the bulk, form stripe or circular domain patterns in two dimensions, as illustrated in Figure 1.5. The stripe pattern results from cylinders lying parallel to the substrate, and a circular domain surface pattern occurs when cylinders are oriented perpendicular to the substrate, or for spheres at the surface. Bicontinuous structures cannot exist in two dimensions, therefore the gyroid phase is suppressed in thin films. More complex multiple stripe and multiple circular domain structures can be formed at the surface of ABC triblocks [81]. Nanostructures in block copolymer films can be oriented using electric fields (if the difference in dielectric permittivity is sufficient), which will be important in applications where parallel stripe [82] or perpendicular cylinder configurations [83] are desired.

The morphology of block copolymers on patterned substrates has attracted recent experimental [84,85] and theoretical [86–88] attention. It has been shown that block copolymer stripes are commensurate with striped substrates if the mismatch in the two lengthscales is not too large.

The surface morphology of block copolymer films can be investigated by atomic force microscopy. The ordering perpendicular to the substrate can be probed by secondary ion mass spectroscopy or specular neutron or X-ray reflectivity. Suitably etched or sectioned samples can be examined by transmission electron microscopy. Islands or holes can have dimensions of micrometers, and consequently may be observed using optical microscopy.

Theory for block copolymer films has largely focused on the ordering of lamellae as a function of film thickness. Many studies have used brush theories

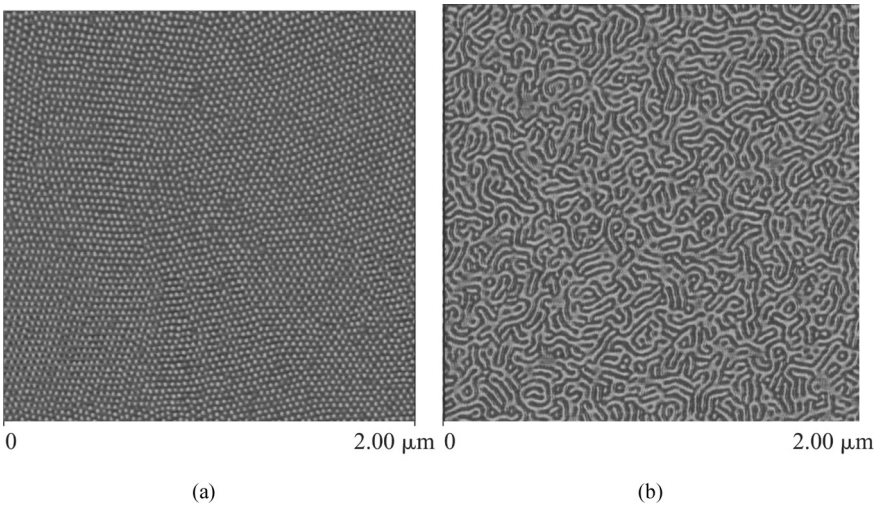

Figure 1.5 Hexagonal and stripe patterns observed via atomic force microscopy (Tapping Mode™). Phase contrast images of (a) polystyrene-*b*-poly(ethylene-co-butylene)-*b*-polystyrene Kraton G1657, (b) Kraton G1650 [210].

for block copolymers in the strong-segregation limit [89,90], although self-consistent field theory has also been employed [68,87,91]. Theory for weakly segregated block copolymers has been applied to analyse surface-induced order above and below the bulk order–disorder transition of a lamellar phase [92] and surface-induced layering in a hexagonal block copolymer film [93]. Computer simulations using the dynamic self-consistent mean-field method have predicted a range of "perforated lamellar" morphologies [94].

1.5 BLOCK COPOLYMERS IN SOLUTION

In a solvent, block copolymer phase behaviour is controlled by the interaction between the segments of the polymers and the solvent molecules as well as the interaction between the segments of the two blocks. If the solvent is unfavourable for one block this can lead to micelle formation in dilute solution. The phase behaviour of concentrated solutions can be mapped onto that of block copolymer melts [95]. Lamellar, hexagonal-packed cylinder, micellar cubic and bicontinuous cubic structures have all been observed (these are all lyotropic liquid-crystal phases, similar to those observed for nonionic surfactants). This is illustrated by representative phase diagrams for Pluronic triblocks in Figure 1.6.

The main classes of block copolymer examined in solution are those based on polyoxyethylene, which is water soluble and is the basis of most amphiphilic block copolymers, and styrenic block copolymers in organic solvents. Selected studies on these systems up to 1998 have been summarized [1]. Polyoxyethylene-based block copolymers include those of polyoxyethylene (E) with polyoxypropylene (P), especially EPE triblocks (commercial name: Pluronic or Synperonic), which are widely used commercially as surfactants in detergents and personal care products [96], and also in pharmaceutical applications, especially drug delivery [97–99]. A number of edited books on water-soluble polymers cover applications of block copolymers [100–105]. Related copolymers include those with a polyoxybutylene hydrophobic block [106,107]. Work on styrenic block copolymers in organic solvents has also been reviewed [1,108]. Block copolymers containing a polyelectrolyte chain have attracted attention from a number of research teams [109,110] (and references therein), copolymers containing a well-studied polyelectrolyte such as poly(styrene sulphonate) [111] or a polyacrylate [109] often being chosen.

Like surfactants, block copolymers form micelles above a critical concentration. The critical micelle concentration can be located by a variety of techniques [112], the most commonly used being surface tensiometry where the cmc is located as the point at which the surface tension becomes essentially independent of concentration. The primary methods to determine micelle size and shape are light scattering and small-angle X-ray and neutron scattering. The thermodynamic radius (from the thermodynamic volume, which is one eighth

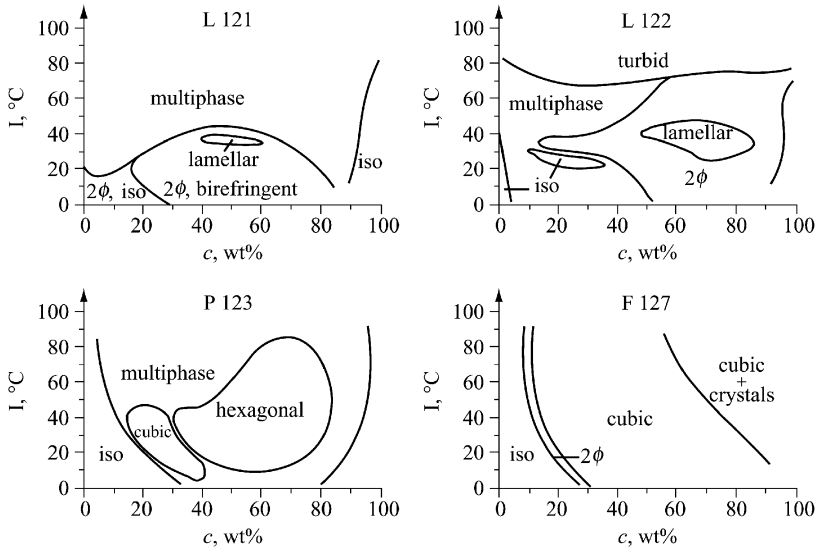

Figure 1.6 Phase diagrams in water of $E_mP_nE_m$ (E=polyoxyethylene, P=polyoxypropylene) Pluronics with $n = 69$ and $m = 4$ (Pluronic L121), $m = 11$ (Pluronic L122), $m = 20$ (Pluronic P123) and $m = 99$ (Pluronic F127). (Reproduced from G. Wanka *et al.* Macromolecules **27**, 4145 (1994). Copyright (1994) with permission from the American Chemical Society.)

of the excluded volume) of micelles can be obtained from static light scattering experiments by fitting the Debye function to the Carnahan–Starling equation for hard spheres [107]. This procedure can be used in place of Zimm plots when the angular dependence of the scattered intensity is weak, which is usually the case for block copolymer micelles, which are much smaller than the wavelength of light [107]. Static light scattering also provides the association number (from the micellar mass) and the second virial coefficient [1,107,113]. Dynamic light scattering provides the hydrodynamic radius from the mode corresponding to micellar diffusion obtained from the intensity distribution of relaxation times (often obtained from analysis of the intensity autocorrelation function using the program CONTIN (114)). The Stokes–Einstein equation can then be used to calculate the hydrodynamic radius from the diffusion coefficient [1,107]. Small-angle X-ray scattering or neutron scattering can be used to extract information on intra- and inter-micellar ordering [1]. Neutron scattering has the advantage compared to X-ray scattering that the contrast between different parts of the system (e.g. within the micelle or between the micelle and the solvent) can be varied by selective deuteration of solvent and/or one of the blocks. In dilute solution, only intramicellar structure contributes to the scattered intensity (the so-called form factor) and this can be modelled to provide information on micelle size and shape. The simplest model is that of a uniform hard sphere [115], although more sophisticated models are usually required for high-quality

data fitting [115–118]. The intermicellar structure factor dominates at higher concentrations. It can be analysed using the hard sphere model [115,119,120] to give information on the micellar radius, and the micellar volume fraction. Where attractive interactions between micelles are significant, these also influence the structure factor and this can be modelled using the "sticky sphere" approximation [117].

A diverse range of theoretical approaches have been employed to analyse the structure of block copolymer micelles, and for micelle formation [1]. The first models were based on scaling relationships for polymer "brushes" and give predictions for the dependence of micelle dimensions on the size of the blocks, as well as the association number of the micelle. A "brush" theory by Leibler and coworkers [121] enables the calculation of the size and number of chains in a micelle and its free energy of formation. The fraction of copolymer chains aggregating into micelles can also be obtained. Self-consistent field theory was first applied to predict the cmc of a diblock in a homopolymer matrix, and then applied to block copolymers in solution. The lattice implementation of SCF theory has been applied by Linse and coworkers [122] to analyse the dimensions of micelles for specific (Pluronic) block copolymers.

In addition to applications as surfactants and in personal care products, block copolymer micelles have been extensively investigated as nanoparticles for solubilizing active agents for drug delivery [97,98,123,124], or as "nanoreactors" for the production of inorganic nanoparticles, e.g. of metals with potential applications in catalysis [125,126]. An alternative approach is to form vesicles (bilayers wrapped round into a spherical shell) [127,128]. These may be crosslinked or polymerized to form hollow-shell nanoparticles [129–131].

At higher concentrations, block copolymers in solution form a variety of lyotropic mesophases [1,132–135]. Due to fact that such phases possess a finite yield stress and so usually do not flow under their own weight, these are often termed gels. However, it must be emphasized that the gel properties result from the ordered microstructure rather than any crosslinks between polymer chains as in a conventional polymer gel. The symmetry of the ordered phase formed largely depends on the interfacial curvature, as for conventional amphiphiles [112], however, the phase behaviour can also be understood by mapping it onto that for block copolymer melts [95]. Shear can be used to orient block copolymer gels as for block copolymer melts. The effects of shear on lyotropic lamellar, hexagonal-packed cylindrical micellar and cubic micellar phases have all been investigated [132,136,137]. Large-amplitude oscillatory shear or high shear rate steady shear both lead to macroscopic orientation of the structures. In the case of cubic phases in particular the flow mechanisms are complex, as is the rheological behaviour with interesting nonlinear effects such as plateaus in the flow curve [138,139].

Theory for the phase behaviour of block copolymers in semidilute or concentrated solution is less advanced than that for melts or dilute solutions due to the complexity of interactions between polymer and solvent. The two main

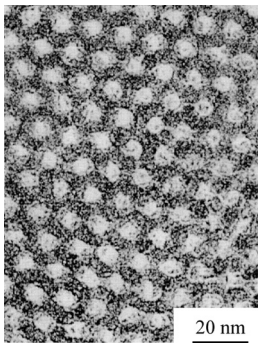

Figure 1.7 TEM image of calcined silica structure templated using an acidic solution of Pluronic poly(oxyethylene)-*b*-poly(oxypropylene)-*b*-poly(oxyethylene) triblock (Reproduced from D. Zhao *et al*. Science **279**, 548 (1998) Copyright (1998) with permission from the American Association for the Arrangement of Science.)

methods developed have been (a) SCF theory for density profiles and domain spacing scalings and (b) weak-segregation limit calculations of the shift in the order–disorder transition temperature with changing concentration. An overview of both approaches can be found elsewhere [1]. SCF theory calculations by Linse and coworkers [140,141] have produced phase diagrams for specific Pluronic copolymers in aqueous solution that are in remarkably good agreement with those observed experimentally. Simulations using the dynamic density functional theory (commercially available as the Mesodyn module of Cerius^2 from Accelerys) have also yielded surprisingly accurate predictions for the sequence of phases obtained on varying concetration [142].

Lyotropic block copolymer mesophases can be used to template inorganic materials such as silica [144, 212], this producing materials with a high internal surface area that could be useful in catalysis or separation technology. Figure 1.7 shows a transmission electron micrograph of hexagonal mesoporous silica, templated using a Pluronic block copolymer.

1.6 CRYSTALLIZATION IN BLOCK COPOLYMERS

In semicrystalline block copolymers, the presence of a noncrystalline block enables modification of the mechanical and structural properties compared to a crystalline homopolymer, through introduction of a rubbery or glassy component. Crystallization in homopolymers leads to an extended conformation, or to *kinetically controlled* chain folding. In block copolymers, on the other hand, *equilibrium* chain folding can occur, the equilibrium number of folds being controlled by the size of the second, noncrystallizable block. The structure of block copolymers following crystallization has been reviewed [1,145].

The most important crystallizable block copolymers are those containing polyethylene or poly(ethylene oxide) (PEO) (systematic name polyoxyethylene). Polyethylene (PE) in block copolymers is prepared by anionic polymerization of poly(1,4-butadiene) (1,4-PB) followed by hydrogenation, and has a melting point in the range 100–110 °C. This synthesis method leads to ethyl branches in the copolymer, with on average 2–3 branches per 100 repeats. These branches induce lengths for folded chains that are set by the branch density and not by the thermodynamics of crystallization. The melting temperature of PEO in block copolymers is generally lower than that of PEO homopolymer (melting temperature $T_m = 76\,^{\circ}C$ for high molecular weight samples). In contrast to PE prepared by hydrogenation of 1,4-PB, there is usually no chain branching in PEO and the fold length depends on the crystallization procedure. Molecules with 1,2,3 . . . folds can be obtained by varying the crystallization protocol (quench depth, annealing time, etc.). Crystallization has been investigated for other block co-polymers, in particular those containing poly (ε-caprolactone) (PCL) ($T_m = 57\,^{\circ}C$). The morphology in block copolymers where both blocks are crystallizable has also been investigated. It has been found that co-crystallization occurs in diblock copolymers, in contrast to blends of crystallizing homopolymers [146]. However, one block can influence the crystallization of another as shown by studies on polystyrene-*b*-polyethylene-*b*-poly(ε-caprolactone) ABC triblocks [147]. A suppression of the crystallization temperature of the poly(ε-caprolactone) block was noted when the polyethylene block crystals were annealed before crystallization of PCL at lower temperatures [147], this effect being termed "antinucleation".

It is now firmly established that confinement of crystalline stems has a profound influence on crystallization in block copolymers. Confinement can result from the presence of glassy domains or simply strong segregation between domains. In contrast, crystallization can overwhelm microphase separation when a sample is cooled from a weakly segregated or homogeneous melt [148–150]. The lamellar crystallites can then nucleate and grow heterogeneously to produce spherulites [148,151], whereas these are not observed when crystallization is confined to spheres or cylinders. Crystallization confined by glassy blocks leads to a drastic slowdown in crystallization kinetics and a reduction in the corresponding Avrami exponent [152,153]. Poly(ethylene) crystallites in a strongly segregated diblock have been observed to nucleate homogeneously within the PE spheres, leading to first-order kinetics, i.e. exponential growth in the degree of crystallinity [154]. Confined crystallization was first observed for a lamellar phase with glassy lamellae [155,156], and later in cylinders confined in a glassy matrix [157]. Crystallization of the polyethylene matrix in the inverse structure (i.e. a phase containing rubbery or glassy cylinders) occurs without disrupting the melt microstructure [158].

Chain folds can exist in equilibrium in block copolymers, in contrast to homopolymers, due to the finite cross sections of the blocks at the lamellar interface, which have to be matched if space is to be filled at normal densities.

The equilibrium fold diagram has been mapped out for poly(ethylene oxide)-based block copolymers in the melt [159] and in solution [160]. Nonequilibrium states of highly folded chains can also be trapped kinetically [160,161].

The orientation of crystalline stems in block copolymers depends on the morphology of the structure and the crystallization protocol. A parallel orientation of polyethylene stems with respect to a lamellar interface was reported for a series of polyethylene-*b*-polyethylethylene diblocks [162], and a similar orientation was later reported by Hamley *et al*. [155,156] for a series of PE-containing diblocks based on simultaneous SAXS/WAXS experiments, as shown in Figure 1.8. SAXS on aligned specimens gives the lamellar orientation, whereas WAXS provides information on unit cell orientation. Samples may be aligned in the melt, for example using large-amplitude oscillatory shear [155,163]. In constrast to these studies showing parallel stem orientation, Rangarajan *et al*. [148] proposed a perpendicular orientation of PE stems in a series of polyolefin diblocks investigated by them. Again using the combination of SAXS and WAXS, Quiram *et al*. [164] found that PE stems generally orient perpendicular to the cylinder axis, although tilted stems were observed when crystallization was confined by strong segregation or by a glassy matrix. These apparently conflicting observations of parallel and perpendicular stem orientations can be rationalised when it is recognised that in both orientations the *b* axis of the PE crystals is the fast growth direction – in the lamellar plane and along the cylinder axis, respectively. Recently, Zhu *et al*. [163] investigated the orientation of PE stems in a PS-b-PEO diblock forming a lamellar phase using SAXS and WAXS. Four regimes were identified: (i) A random stem orientation for a deep quench into liquid nitrogen, (ii) stems parallel to lamellae for a crystallization temperature $-50 \leq T_c \leq -10^{\circ}C$, (iii) Stems inclined with respect to lamellae were observed for $-5 \leq T_c \leq -30^{\circ}C$, (iv) Stems perpendicular to

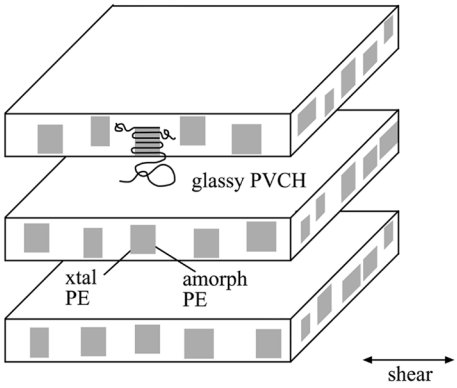

Figure 1.8 Model for confined crystallization in a lamellar phase formed by a polyethylene-*b*-poly(vinylcyclohexane) diblock (Reproduced from I. W. Hamley *et al*. Macromolecules **29**, 8835 (1996) Copyright (1996) with permission from the American Chemical Society.)

lamellae were observed for $T_c \geq 35°C$ [163]. For PEO cylinders formed in a PS-PEO diblock the parallel orientation of stems was not observed, although the states (i), (iii) and (iv) were confirmed [165]. These conclusions were supported by a separate study of the correlation lengths (apparent crystallite sizes) obtained from SAXS for different crystal orientations [166]. In this report it was also noted that it is the initial growth stage that determines the final crystal orientation in nanoconfined lamellae rather than the primary nucleation step. Crystal orientation and changes in lamellar thickness of a related diblock were examined in a companion paper, in which the change in the crystallization kinetics for confined and unconfined crystallization were deduced from Avrami plots of the degree of crystallinity [167].

Theories for semicrystalline block copolymers are able to provide predictions for the scaling of amorphous and crystal layer thickness with chain length [1,145]. A brush-type theory was developed by DiMarzio *et al.* [168] and a self-consistent field theory by Whitmore and Noolandi [169]. The latter approach predicts a scaling for the overall domain spacing $d \sim NN_a^{-5/12}$ (where N is the total degree of polymerization and N_a is that of the amorphous block) that is in good agreement with experimental results [170], as detailed elsewhere [1,145]. Approaches used for crystallization in homopolymers may be used to calculate the change in melting temperature due to finite crystal thickness (Thompson–Gibbs equation), lamellar crystal surface energies (Flory–Vrij theory), and growth rates (kinetic nucleation theory). Details can be obtained from [1].

The morphology of thin films of crystallized block copolymers can be probed most conveniently at the microscopic scale by atomic force microscopy (AFM), whereas spherulites can be observed optically. Crystallization in thin films of PE-*b*-PEO diblocks has recently been investigated by Reiter and coworkers [171,172]. For a diblock containing 45% PEO they observed, using AFM, parallel lamellae in the melt but lamellae oriented perpendicular to the substrate upon crystallization at a large undercooling [172]. This was ascribed to a kinetically trapped state of chain-folded PEO crystals. However, ultimately the morphology evolved into the equilibrium parallel one, which was also observed for three other diblocks with a higher PEO content [172]. Films of these copolymers were characterized by islands and holes at the surface due to an incommensurability between the film thickness and an integral number of lamellae, as discussed in Section 1.4. The island and hole structure was retained upon crystallization, although craters and cracks appeared in the lamellae. Within craters, terracing of lamellar steps was observed, from which the lamellar thickness could be extracted. Terracing of crystal lamellae oriented parallel to the substrate was also reported for a PEO-*b*-PBO diblock and a PEO-*b*-PBO-*b*-PEO triblock, probed via AFM [173]. In this work a comparison of the lamellar thickness was also made with the domain spacing obtained from SAXS and a model of tilted chains was proposed (fully extended for the diblock, once folded for the triblock). However, this is

not in agreement with recent simultaneous SAXS/WAXS results that indicate PEO chains oriented perpendicular to lamellae in a PEO-*b*-PBO diblock [174].

1.7 BLENDS CONTAINING BLOCK COPOLYMERS

In blends of block copolymer with homopolymer, there is an interplay between macrophase separation (due to the presence of homopolymer) and microphase separation (of the block copolymer). Which effect predominates depends on the relative lengths of the polymers, and on the composition of the blend.

Macrophase separation can be detected by light scattering or via turbidity measurements of the cloud point since macrophase separation leads to structures with a length scale comparable to that of the wavelength of light. Regions of macrophase and microphase separation can also be distinguished by transmission electron microscopy or via small-angle scattering techniques. Microphase separation leads to a scattering peak at a finite wavenumber q, whereas macrophase separation is characterized by $q = 0$. The segregation of block copolymers to the interface between polymers in a blend can be determined in bulk from small-angle scattering experiments or TEM. In thin films, neutron reflectivity, forward recoil spectroscopy and nuclear reaction analysis have been used to obtain volume fraction profiles, which quantify the selective segregation of block copolymers to interfaces.

An important application of block copolymers is as compatibilizers of otherwise immiscible homopolymers. There are a number of useful reviews of work in this area [175–178]. The morphology of blends of polymers with block copolymer, and theories for this, have been reviewed [1]. The influence of added homopolymer on block copolymer structure has also been investigated, as have binary blends of block copolymers, and these systems are also considered in this section.

1.7.1 BLENDS OF BLOCK COPOLYMER WITH ONE HOMOPOLYMER

Block copolymers can solubilize homopolymers up to a certain amount, beyond which phase separation occurs. This ability to continuously swell block copolymer microstructures is the basis of a number of potential and actual applications in optoelectonics where the periodicity of the block copolymer structure is extended up to 0.1–1 μm, which corresponds to wavelengths for reflection or guiding of light. The limit for macrophase separation in blends of block copolymer with homopolymer depends on the relative chain lengths, i.e. on $\alpha = N_{Ah}/N_{Ac}$, where N_{Ah} is the degree of polymerization of the homopolymer (A) and N_{Ac} is the degree of polymerisation of the same component of the

copolymer. Work by the groups of Hashimoto [179] and Winey [180–182] has led to the identification of three regimes [1]. If $\alpha < 1$, the homopolymer tends to be selectively solubilized in the A domain of the microphase-separated block copolymer, and is weakly segregated towards the domain centre. If $\alpha \approx 1$, the homopolymer is still selectively solubilized in the A microdomains. However, it does not significantly swell the A block chains and tends to be more localized in the middle of the A microdomains. If $\alpha > 1$, macrophase separation occurs, with domains of microphase-separated copolymer in the homopolymer matrix. A transmission electron micrograph of the structure formed by a phase-separated lamellar diblock is shown in Figure 1.9.

Another important aspect of adding homopolymer to a block copolymer is the ability to change morphology (without synthesis of additional polymers). Furthermore, morphologies that are absent for neat diblocks such as bicontinuous cubic "double diamond" or hexagonal-perforated layer phases have been predicted in blends with homopolymers [183], although not yet observed. Transitions in morphology induced by addition of homopolymer are reviewed elsewhere [1], where a list of experimental studies on these systems can also be found.

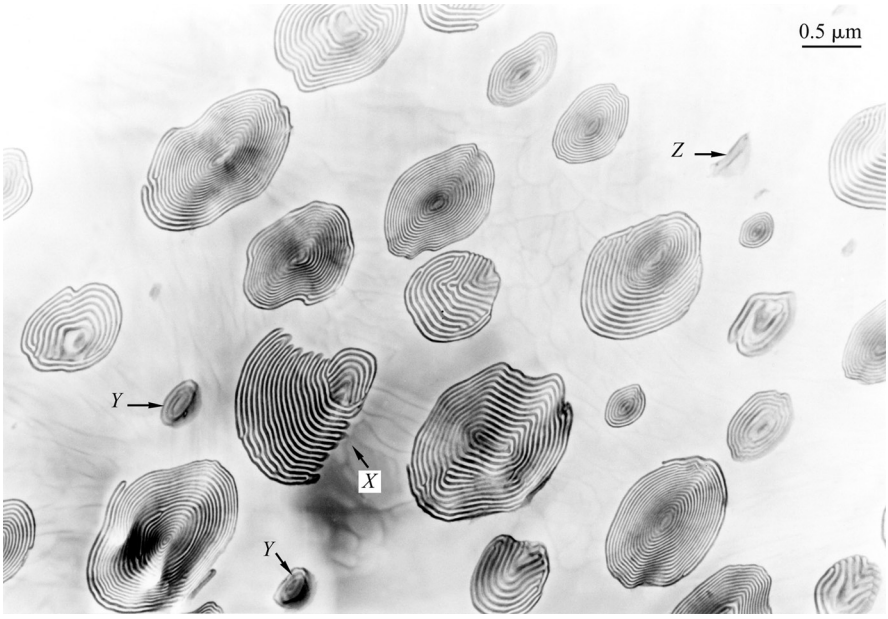

Figure 1.9 Electron micrograph showing macrophase separation of domains of microphase-separated polystyrene-*b*-polyisoprene block copolymer ($M_n = 100\,kg\,mol^{-1}$, $f_{PS} = 0.46$) in a PS homopolymer ($M_n = 580\,kg\,mol^{-1}$) matrix (Reproduced from S. Koizumi *et al.* Macromolecules **27**, 6532 (1994) Copyright (1994) with permission from the American Chemical Society.)

1.7.2 BLENDS OF BLOCK COPOLYMER WITH TWO HOMOPOLYMERS

The ability of block copolymers to act as compatibilizers is now established. However, a debate has occurred in the literature as to whether block copolymers are more effective compatibilizers than random copolymers. For example, it has been reported that polystyrene/poly(2-vinylpyridine) random copolymers act to compatibilize the parent homopolymers [184], but that random polystyrene/poly(methyl methacrylate) copolymers are much less effective than block copolymers [185]. The key appears to be the blockiness of the copolymer, which is much higher for the latter [186]. Theory suggests that compositional polydispersity is also important for effective compatibilization [186,187]. It leads to a greater gradation in composition across the interface, and consequently a lower configurational entropy of the homopolymers [187]. In practice, polymers are compatibilized during melt processing. Then kinetic quantities such as the rate of diffusion of the copolymers to the interface and the shear rate are important. Macosko and coworkers [188] have shown that the coalescence of polymer droplets is inhibited by diffusion of block copolymers. The molar mass must be low enough so that diffusion occurs rapidly but not too low to prevent entanglements at the interface. On the other hand, copolymers with a molar mass that is too high get stuck in micelles.

Block copolymers act as compatibilizers by reducing the interfacial tension between homopolymers. Recent work shows that block copolymers can reduce the interfacial tension between homopolymers to the extent that polymeric microemulsions can be formed where the copolymer forms a continuous film between spatially continuous homopolymer domains [189–191]. A TEM image of a microemulsion formed in a blend of two polyolefins and the corresponding symmetric diblock is shown in Figure 1.10. A bicontinuous microemulsion forms in the mixture composition range where mean-field theory predicts a Lifshitz point [192]. A Lifshitz point is defined as the point along the line of critical phase transitions at which macro- and microphase branches meet [1]. The observation of a microemulsion shows that mean-field theory breaks down due to the existence of thermal composition fluctuations. Although a theory for these composition fluctuations has not yet been developed, it has been shown that some properties of the microemulsion (elastic constants, composition profiles) can be modelled using an approach where the effective interaction between copolymer monolayers is computed [187,193,194]. Both SCF and SSL theories have been employed [194]. The effect of shear on polymeric microemulsions has recently been investigated, and it was shown that macrophase separation can be induced at sufficiently high shear rates [195]. The connection between microemulsions formed by block copolymers and those containing conventional amphiphilies (which can be used to stabilize oil/water mixtures) has been emphasized [190,196] due to the importance of this aspect of block copolymer phase behaviour to applications.

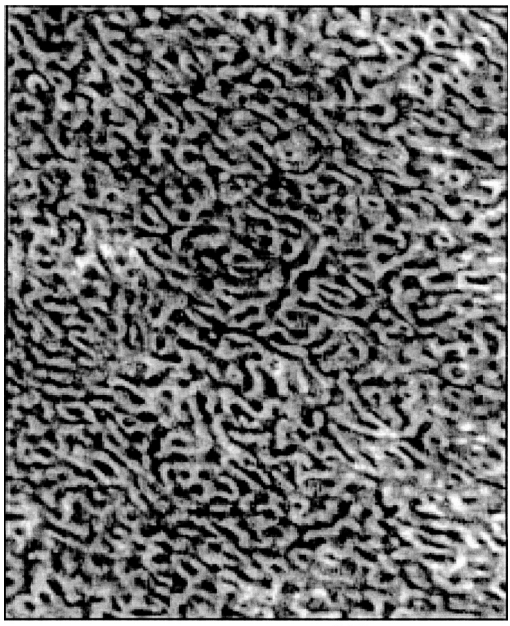

Figure 1.10 Transmission electron micrograph image of a microemulsion formed in a ternary blend of polyethylene, poly(ethylene-propylene) and a symmetric diblock of these two polymers (Reproduced from M. A. Hillmyer *et al*. J. Phys. Chem. B **103**, 4814 (1999) Copyright (1999) with permission from the American Chemical Society.)

1.7.3 BLENDS OF BLOCK COPOLYMERS

Macro-versus micro-phase separation in blends of block copolymers has been investigated in particular for blends of polystyrene-*b*-polyisoprene diblock copolymers by Hashimoto and coworkers [197–201]. Writing the ratio of chain lengths as $\delta = N_1/N_2$, it was found that blends of lamellar diblocks are miscible for $\delta < 5$, whereas for $\delta > 5$, the mixtures are only partially miscible [197,200]. The same limiting value of δ was obtained by Matsen using self-consistent mean-field calculations [202]. The miscibility of pairs of asymmetric diblocks with the same [198] or complementary [198,199,203] compositions has also been investigated. By blending complementary diblocks (i.e. those with composition f and $1–f$), it is possible to induce a lamellar phase even for mixtures of asymmetric diblocks forming cylinder phases when pure [198,203]. Blends of diblocks with similar compositions and molecular weights can be used to map the phase diagram by interpolation in the composition range spanned [143]. By blending, the synthesis requirements to obtain a full phase diagram are reduced. The validity of this so-called "single-component" approximation has been tested using SCF theory. It was found that phase

boundaries in the (f_1, f_2) plane, where f_1 and f_2 are the compositions of the two diblocks) map onto those of the corresponding pure diblock, at least if f_1 and f_2 do not differ too much [204,205]. In the case that either f_1 or f_2 becomes close to zero or unity, this approximation completely breaks down [205]. Thus, the one-component approximation is useful, although evidently the phase diagram of binary blends will contain biphasic regions.

Motivated by the possibility to prepare "exotic morphologies" exhibited by ABC triblocks just by blending diblocks, Frielinghaus *et al*. [206,207] have investigated phase diagrams of strongly interacting AB and BC diblocks where the common B block is polyisoprene and the other two blocks are polystyrene and poly(ethylene oxide). Although exotic phases were not found, regions of miscibility and immiscibility were mapped out. The phase diagrams obtained were in surprisingly good agreement with the predictions of a simple random-phase approximation calculation of the spinodals [208].

REFERENCES

1. I. W. Hamley, *The Physics of Block Copolymers* (Oxford University Press, Oxford, 1998].
2. P. Alexandridis and J. F. Holzwarth, *Curr. Opin. Colloid Interface Sci*. **5**, 312 (2000).
3. N. Hadijichristidis, S. Pispas and G. A. Floudas *Block Copolymers* (Wiley, New York, 2003).
4. G. Riess, G. Hurtrez, and P. Bahadur, in *Encyclopedia of Polymer Science and Engineering*, edited by H. F. Mark and J. I. Kroschwitz (Wiley, New York, 1985), Vol. 2, p. 324.
5. M. Hillmyer, *Curr. Opin. Solid State Mater. Sci*. **4**, 559 (1999).
6. M. Scwarc, M. Levy, and R. Milkovich, *J. Am. Chem. Soc*. **78**, 2656 (1956).
7. R. N. Young, R. P. Quirk, and L. J. Fetters, *Adv. Polym. Sci*. **56**, 1 (1985).
8. P. Rempp, E. Franta, and J. Herz, *Adv. Polym. Sci*. **86**, 147 (1989).
9. M. van Beylen, S. Bywater, G. Smets, M. Szwarc, and D. Worsfold, *Adv. Polym. Sci*. **86**, 89 (1989).
10. H. L. Hsieh and R. P. Quirk, *Anionic Polymerization: Principles and Practical Applications* (Marcel Dekker, New York, 1996).
11. N. Hadjichristidis, H. Iatrou, S. Pispas, and M. Pitsikalis, *J. Polym. Sci.A: Polym. Chem*. **38**, 3211 (2000).
12. M. Pitsikalis, S. Pispas, J. W. Mays, and N. Hadjichristidis, *Adv. Polym. Sci*. **135**, 1 (1998).
13. N. Hadjichristidis, *J. Polym. Sci.A: Polym. Chem*. **37**, 857 (1999).
14. N. Hadjichristidis, N. Pispas, M. Pitsikalis, H. Iatrou, and C. Vlahos, *Adv. Polym. Sci*. **142**, 71 (1999).
15. Z.-G. Yan, Z. Yang, C. Price, and C. Booth, *Makromol. Chem., Rapid Commun*. **14**, 725 (1993).
16. K. Matyjaszewski and J. Xia, *Chem. Rev*. **101**, 2921 (2001).
17. K. A. Davis and K. Matyjaszewski, *Macromolecules* **34**, 2101 (2001).
18. J. P. Kennedy and E. Maréchal, *Carbocationic Polymerization* (Wiley, New York, 1982).
19. J. P. Kennedy and B. Ivan, *Designed Polymers by Carbocationic Macromolecular Engineering: Theory and Practice* (Hanser, Munich, 1992).

20. M. Sawamoto and M. Kamigaito, in *New Methods of Polymer Synthesis*, edited by J. R. Ebdon and G. C. Eastmond (Blackie, London, 1995), Vol. 2.
21. S. T. Nguyen, L. K. Johnson, R. H. Grubbs, and J. W. Ziller, *J. Am. Chem. Soc*. **114**, 3975 (1992).
22. M. J. Folkes and A. Keller, in *The Physics of Glassy Polymers*, edited by R. N. Haward (Applied Science, London, 1973), p. 548.
23. F. S. Bates and G. H. Fredrickson, *Ann. Rev. Phys. Chem*. **41**, 525 (1990).
24. F. S. Bates and G. H. Fredrickson, *Physics Today* **52,** Feb issue, 32 (1999).
25. G. H. Fredrickson and F. S. Bates, *Annu. Rev. Mater. Sci*. **26**, 501 (1996).
26. R. H. Colby, *Curr. Opin. Colloid Interface Sci*. **1**, 454 (1996).
27. D. A. Hajduk, P. E. Harper, S. M. Gruner, C. C. Honeker, G. Kim, E. L. Thomas, and L. J. Fetters, *Macromolecules* **27**, 4063 (1994).
28. S. Förster, A. K. Khandpur, J. Zhao, F. S. Bates, I. W. Hamley, A. J. Ryan, and W. Bras, *Macromolecules* **27**, 6922 (1994).
29. I. W. Hamley, K. A. Koppi, J. H. Rosedale, F. S. Bates, K. Almdal, and K. Mortensen, *Macromolecules* **26**, 5959 (1993).
30. D. A. Hajduk, H. Takenouchi, M. A. Hillmyer, F. S. Bates, M. E. Vigild, and K. Almdal, *Macromolecules* **30**, 3788 (1997).
31. M. E. Vigild, K. Almdal, K. Mortensen, I. W. Hamley, J. P. A. Fairclough, and A. J. Ryan, *Macromolecules* **31**, 5702 (1998).
32. M. F. Schulz and F. S. Bates, in *Physical Properties of Polymers Handbook*, edited by J. E. Mark (American Institute of Physics, Woodbury, New York, 1996), p. 427.
33. K. Kato, *J. Electron Microsc*. (Japan) **14**, 220 (1965).
34. P. M. Lipic, F. S. Bates, and M. W. Matsen, *J. Polym. Sci. B: Polym. Phys*. **37**, 2229 (2001).
35. F. S. Bates, J. H. Rosedale, and G. H. Fredrickson, *J. Chem. Phys*. **92**, 6255 (1990).
36. J. H. Rosedale and F. S. Bates, *Macromolecules* **23**, 2329 (1990).
37. C. D. Han, D. M. Baek, J. K. Kim, T. Ogawa, N. Sakamoto, and T. Hashimoto, *Macromolecules* **28**, 5043 (1995).
38. S. M. Mai, J. P. A. Fairclough, I. W. Hamley, R. C. Denny, B. Liao, C. Booth, and A. J. Ryan, *Macromolecules* **29**, 6212 (1996).
39. N. Sakamoto and T. Hashimoto, *Macromolecules* **28**, 6825 (1995).
40. V. P. Voronov, V. M. Buleiko, V. E. Podneks, I. W. Hamley, J. P. A. Fairclough, A. J. Ryan, S.-M. Mai, B.-X. Liao, and C. Booth, *Macromolecules* **30**, 6674 (1997).
41. E. Helfand and A. M. Sapse, *J. Chem. Phys*. **62**, 1327 (1975).
42. F. S. Bates and G. H. Fredrickson, *Macromolecules* **27**, 1065 (1994).
43. G. H. Fredrickson and E. Helfand, *J. Chem. Phys*. **87**, 697 (1987).
44. G. H. Fredrickson and K. Binder, *J. Chem. Phys*. **91**, 7265 (1989).
45. E. Helfand, *Macromolecules* **8**, 552 (1975).
46. E. Helfand and Z. R. Wasserman, *Macromolecules* **9**, 879 (1976).
47. E. Helfand and Z. R. Wasserman, in *Developments in Block Copolymers 1*, edited by I. Goodman (Applied Science, London, 1982), p. 99.
48. L. Leibler, *Macromolecules* **13**, 1602 (1980).
49. M. W. Matsen and M. Schick, *Phys. Rev. Lett*. **72**, 2660 (1994).
50. M. W. Matsen and M. Schick, *Curr. Opin. Colloid Interface Sci*. **1**, 329 (1996).
51. M. W. Matsen and F. S. Bates, *Macromolecules* **29**, 1091 (1996).
52. M. W. Matsen, *J. Phys. Condens. Matter*, **14**, R21 (2001).
53. E. F. David and K. S. Schweizer, *J. Chem. Phys*. **100**, 7767 (1994).
54. E. F. David and K. S. Schweizer, *J. Chem. Phys*. **100**, 7784 (1994).
55. V. Ganesan and G. H. Fredrickson, *Europhys. Lett*. **55**, 814 (2001).
56. A. J. Ryan and I. W. Hamley, in *The Physics of Glassy Polymers*, edited by R. N. Haward and R. J. Young (Chapman and Hall, London, 1997).

57. F. Drolet and G. H. Fredrickson, *Phys. Rev. Lett*. **83**, 4317 (1999).
58. Y. Bohbot-Raviv and Z.-G. Wang, *Phys. Rev. Lett*. **85**, 3428 (2000).
59. A. Keller, E. Pedemonte, and F. M. Willmouth, *Nature* **225**, 538 (1970).
60. C. C. Honeker and E. L. Thomas, *Chem. Mater*. **8**, 1702 (1996).
61. I. W. Hamley, *J. Phys. Condens. Matter* **13**, R643 (2001).
62. K. A. Koppi, M. Tirrell, F. S. Bates, K. Almdal, and R. H. Colby, *J. Phys. France* II **2**, 1941 (1992).
63. K. A. Koppi, M. Tirrell, and F. S. Bates, *Phys. Rev. Lett*. **70**, 1449 (1993).
64. K. Almdal, K. Mortensen, K. A. Koppi, M. Tirrell, and F. S. Bates, *J. Phys. France* II **6**, 617 (1996).
65. A. Nakajima, T. Hayashi, K. Kugo, and K. Shinoda, *Macromolecules* **12**, 840 (1979).
66. A. Nakajima, K. Kugo, and T. Hayashi, *Macromolecules* **12**, 844 (1979).
67. J. J. L. M. Cornelissen, M. Fischer, N. A. J. M. Sommerdijk, and R. J. M. Nolte, *Science* **280**, 1427 (1998).
68. M. W. Matsen, *J. Chem. Phys*. **106**, 7781 (1997).
69. K. Liu, S. M. Baker, M. Tuominen, T. P. Russell, and I. K. Schuller, *Phys. Rev. B* **63**, 060403(R) (2001).
70. M. Park, C. Harrison, P. M. Chaikin, R. A. Register, and D. H. Adamson, *Science* **276**, 1401 (1997).
71. C. Harrison, M. Park, P. M. Chaikin, R. A. Register, and D. H. Adamson, *J. Vac. Sci. Technol. B* **16**, 544 (1998).
72. G. Widawski, M. Rawiso, and B. François, *Nature* **369**, 387 (1994).
73. M. W. Matsen, *Curr. Opin. Colloid Interface Sci*. **3**, 40 (1998).
74. K. E. Strawhecker, S. K. Kumar, J. F. Douglas, and A. Karim, *Macromolecules* **34**, 4669 (2001).
75. A. Böker, A. H. E. Müller, and G. Krausch, *Macromolecules* **34**, 7477 (2001).
76. I. W. Hamley, E. L. Hiscutt, Y.-W. Yang, and C. Booth, *J. Colloid Interface Sci*. **209**, 255 (1999).
77. R. Limary and P. F. Green, *Langmuir* **15**, 5617 (1999).
78. P. Müller-Buschbaum, J. S. Gutmann, and M. Stamm, *Phys. Chem., Chem. Phys*. **1**, 3857 (1999).
79. D. Ausserré, D. Chatenay, G. Coulon, and R. Collin, *J. Phys. France* **51**, 2571 (1990).
80. S. H. Anastasiadis, T. P. Russell, S. K. Satija, and C. F. Majkrzak, *Phys. Rev. Lett*. **62**, 1852 (1989).
81. N. Rehse, A. Knoll, M. Konrad, R. Magerle, and G. Krausch, *Phys. Rev. Lett*. **87**, 035505 (2001).
82. T. L. Morkved, M. Lu, A. M. Urbas, E. E. Ehrichs, H. M. Jaeger, P. Mansky, and T. P. Russell, *Science* **273**, 931 (1996).
83. T. Thurn-Albrecht, J. Schotter, G. A. Kästle, N. Emley, T. Shibauchi, L. Krusin-Elbaum, K. Guarini, C. T. Black, M. T. Tuominen, and T. P. Russell, *Science* **290**, 2126 (2000).
84. L. Rockford, Y. Liu, P. Mansky, T. P. Russell, M. Yoon, and S. G. J. Mochrie, *Phys. Rev. Lett*. **82**, 2602 (1999).
85. X. M. Yang, R. D. Peters, P. F. Nealey, H. H. Solak, and F. Cerrina, *Macromolecules* **33**, 9575 (2000).
86. G. G. Pereira and D. R. M. Williams, *Europhys. Lett*. **44**, 302 (1998).
87. D. Petera and M. Muthukumar, *J. Chem. Phys*. **109**, 5101 (1998).
88. Y. Tsori and D. Andelman, *Europhys. Lett*. **53**, 722 (2001).
89. M. S. Turner, *Phys. Rev. Lett*. **69**, 1788 (1992).
90. D. G. Walton, D. J. Kellogg, A. M. Mayes, P. Lambooy, and T. P. Russell, *Macromolecules* **27**, 6225 (1994).

91. G. T. Pickett and A. C. Balazs, *Macromolecules* **30**, 3097 (1997).
92. G. H. Fredrickson, *Macromolecules* **20**, 2535 (1987).
93. M. S. Turner, M. Rubinstein, and C. M. Marques, *Macromolecules* **27**, 4986 (1994).
94. H. P. Huinink, M. A. van Dijk, J. Brokken-Zijp, and G. J. A. Sevink, *Macromolecules* **34**, 5325 (2001).
95. K. J. Hanley, T. P. Lodge, and C.-I. Huang, *Macromolecules* **33**, 5918 (2000).
96. J. E. Glass, Ed., *Water-soluble Polymers: Beauty with Performance* (American Chemical Society, Washington, D.C., 1986), Vol. 213.
97. I. R. Schmolka, in *Polymers for Controlled Drug Delivery*, edited by P. J. Tarcha (CRC Press, Boston, 1991).
98. M. W. Edens, in *Nonionic Surfactants. Polyoxyalkylene Block Copolymers*, edited by V. N. Nace (Marcel Dekker, New York, 1996), Vol. 60, p. 185.
99. M. Malmsten, in *Amphiphilic Block Copolymers: Self-assembly and Applications*, edited by P. Alexandridis and B. Lindman (Elsevier, Amsterdam, 2000).
100. P. Molyneux, *Water-soluble Synthetic Polymers: Properties and Behavior* (CRC Press, Boca Raton, 1983).
101. S. W. Shalaby, C. L. McCormick, and G. B. Butler, Eds., *Water-soluble Polymers. Synthesis, Solution Properties and Applications* (American Chemical Society, Washington, D.C., 1991), Vol. 467.
102. J. E. Glass, Ed., *Hydrophilic Polymers: Performance with Environmental Acceptability* (American Chemical Society, Washington, D.C., 1996), Vol. 248.
103. V. N. Nace, Ed., *Nonionic Surfactants. Polyoxyalkylene Block Copolymers* (Marcel Dekker, New York, 1996), Vol. 60.
104. P. Alexandridis and B. Lindman, Eds, *Amphiphilic Block Copolymers: Self-assembly and Applications* (Elsevier, Amsterdam, 2000).
105. J. E. Glass, Ed., *Associative Polymers in Aqueous Media* (American Chemical Society, Washington, D.C., 2000), Vol. 765.
106. C. Booth, G.-E. Yu, and V. M. Nace, in *Amphiphilic Block Copolymers: Self-assembly and Applications*, edited by P. Alexandridis and B. Lindman (Elsevier, Amsterdam, 2000), p. 57.
107. C. Booth and D. Attwood, *Macromol. Rapid Comm.* **21**, 501 (2000).
108. Z. Tuzar and P. Kratochvil, in *Surface Colloid Science.*, edited by E. Matijevic (Plenum, New York, 1993), Vol. 15, p. 1.
109. L. Zhang, K. Khougaz, M. Moffitt, and A. Eisenberg, in *Amphiphilic Block Copolymers: Self-assembly and Applications*, edited by P. Alexandridis and B. Lindman (Elsevier, Amsterdam, 2000).
110. K. Szczubialka, K. Ishikawa, and Y. Morishima, *Langmuir* **16**, 2083 (2000).
111. P. Guenoun, M. Delsanti, D. Gazeau, J. W. Mays, D. C. Cook, M. Tirrell, and L. Auvray, *Eur. Phys. J. B* **1**, 77 (1998).
112. I. W. Hamley, *Introduction to Soft Matter* (John Wiley, Chichester, 2000).
113. Z. Tuzar and P. Kratochvil, in *Light Scattering – Principles and Development*, edited by W. Brown (Oxford University Press, Oxford, 1996), p. 327.
114. S. W. Provencher, *Makromol. Chem.* **180**, 201 (1979).
115. J. S. Pedersen, *Adv. Colloid Interface Sci.* **70**, 171 (1997).
116. J. S. Pedersen and M. C. Gerstenberg, *Macromolecules* **29**, 1363 (1996).
117. Y. Liu, S.-H. Chen, and J. S. Huang, *Macromolecules* **31**, 2236 (1998).
118. J. S. Pedersen, *Curr. Opin. Colloid Interface Sci.* **4**, 190 (1999).
119. N. W. Ashcroft and J. Lekner, *Phys. Rev.* **145**, 83 (1966).
120. K. Mortensen and J. S. Pedersen, *Macromolecules* **26**, 805 (1993).
121. L. Leibler, H. Orland, and J. C. Wheeler, *J. Chem. Phys.* **79**, 3550 (1983).
122. P. Linse, *Macromolecules* **26**, 4437 (1993).

123. J. Zipfel, P. Lindner, M. Tsianou, P. Alexandridis, and W. Richtering, *Langmuir* **15**, 2599 (1999).
124. T. Riley, S. Stolnik, C. R. Heald, C. D. Xiong, M. C. Garnett, L. Illum, and S. S. Davis, *Langmuir* **17**, 3168 (2001).
125. M. V. Seregina, L. M. Bronstein, O. A. Platonova, D. M. Chernyshov, P. M. Valetsky, J. Hartmann, E. Wenz, and M. Antonietti, *Chem. Mater*. **9**, 923 (1997).
126. L. M. Bronstein, S. N. Sidorov, P. M. Valetsky, J. Hartmann, H. Cölfen, and M. Antonietti, *Langmuir* **15**, 6256 (1999).
127. L. Zhang, K. Yu, and A. Eisenberg, *Science* **272**, 1777 (1996).
128. L. Luo and A. Eisenberg, *J. Am. Chem. Soc*. **123**, 1012 (2001).
129. S. Stewart and G. Liu, *Chem. Mater*. **11**, 1048 (1999).
130. B. M. Discher, Y.-Y. Won, D. S. Ege, J. C.-M. Lee, F. S. Bates, D. E. Discher, and D. A. Hammer, *Science* **284**, 1143 (1999).
131. C. Nardin, T. Hirt, J. Leukel, and W. Meier, *Langmuir* **16**, 1035 (2000).
132. K. Mortensen, *Curr. Opin. Colloid Interface Sci*. **3**, 12 (1998).
133. P. Alexandridis, U. Olsson, and B. Lindman, *Langmuir* **14**, 2627 (1998).
134. P. Alexandridis and R. J. Spontak, *Curr. Opin. Colloid Interface Sci*. **4**, 130 (1999).
135. K. Mortensen, *Coll. Surf. A* **183–185**, 277 (2001).
136. I. W. Hamley, *Curr. Opin. Colloid Interface Sci*. **5**, 342 (2000).
137. I. W. Hamley, *Philos. Trans. R. Soc. Lond*. **359**, 1017 (2001).
138. E. Eiser, F. Molino, G. Porte, and O. Diat, *Phys. Rev. E* **61**, 6759 (2000).
139. P. Holmqvist, C. Daniel, I. Hamley, W. Mingvanish, and C. Booth, *Colloid Surf*. A, in press (2001).
140. J. Noolandi, A.-C. Shi, and P. Linse, *Macromolecules* **29**, 5907 (1996).
141. M. Svensson, P. Alexandridis, and P. Linse, *Macromolecules* **32**, 637 (1999).
142. B. A. C. van Vlimmeren, N. M. Maurits, A. V. Zvelinodvsky, G. J. A. Sevink, and J. G. E. M. Fraaije, *Macromolecules* **32**, 646 (1999).
143. J. Zhao, B. Majumdar, M. F. Schulz, F. S. Bates, K. Almdal, K. Mortensen, D. A. Hajduk, and S. M. Gruner, *Macromolecules* **29**, 1204 (1996).
144. P. Kipkemboi, A. Fogden, V. Alfredsson, and K. Flodström, *Langmuir* **17**, 5394 (2001).
145. I. W. Hamley, *Adv. Polym. Sci*. **148**, 113 (1999).
146. S. Nojima, M. Ono, and T. Ashida, *Polym. J*. **24**, 1271 (1992).
147. V. Balsamo, A. J. Müller, and R. Stadler, *Macromolecules* **31**, 7756 (1998).
148. P. Rangarajan, R. A. Register, and L. J. Fetters, *Macromolecules* **26**, 4640 (1993).
149. P. Rangarajan, R. A. Register, D. H. Adamson, L. J. Fetters, W. Bras, S. Naylor, and A. J. Ryan, *Macromolecules* **28**, 1422 (1995).
150. A. J. Ryan, I. W. Hamley, W. Bras, and F. S. Bates, *Macromolecules* **28**, 3860 (1995).
151. V. Balsamo, G. Gil, C. Urbina de Navarro, I. W. Hamley, F. von Gyldenfeldt, V. Abetz and E. Cañizales, *Macromolecules* **36**, 4515 (2003).
152. I. W. Hamley, J. P. A. Fairclough, F. S. Bates, and A. J. Ryan, *Polymer* **39**, 1429 (1998).
153. T. Shiomi, H. Tsukuda, H. Takeshita, K. Takenaka, and Y. Tezuka, *Polymer* **42**, 4997 (2001).
154. Y.-L. Loo, R. A. Register, and A. J. Ryan, *Phys. Rev. Lett*. **84**, 4120 (2000).
155. I. W. Hamley, J. P. A. Fairclough, N. J. Terrill, A. J. Ryan, P. M. Lipic, F. S. Bates, and E. Towns-Andrews, *Macromolecules* **29**, 8835 (1996).
156. I. W. Hamley, J. P. A. Fairclough, A. J. Ryan, F. S. Bates, and E. Towns-Andrews, *Polymer* **37**, 4425 (1996).
157. D. J. Quiram, R. A. Register, G. R. Marchand, and A. J. Ryan, *Macromolecules* **30**, 8338 (1997).

158. Y.-L. Loo, R. A. Register, and D. H. Adamson, *Macromolecules* **33**, 8361 (2000).
159. S.-M. Mai, J. P. A. Fairclough, K. Viras, P. A. Gorry, I. W. Hamley, A. J. Ryan, and C. Booth, *Macromolecules* **30**, 8392 (1997).
160. M. Gervais and B. Gallot, *Makromol. Chem*. **171**, 157 (1973).
161. A. J. Ryan, J. P. A. Fairclough, I. W. Hamley, S.-M. Mai, and C. Booth, *Macromolecules* **30**, 1723 (1997).
162. K. C. Douzinas and R. E. Cohen, *Macromolecules* **25**, 5030 (1992).
163. L. Zhu, S. Z. D. Cheng, B. H. Calhoun, Q. Ge, R. P. Quirk, E. L. Thomas, B. S. Hsiao, F. Yeh, and B. Lotz, *J. Am. Chem. Soc*. **122**, 5957 (2000).
164. D. J. Quiram, R. A. Register, and G. R. Marchand, *Macromolecules* **30**, 4551 (1997).
165. P. Huang, L. Zhu, S. Z. D. Cheng, Q. Ge, R. P. Quirk, E. L. Thomas, B. Lotz, B. S. Hsiao, L. Liu, and F. Yeh, *Macromolecules* **34**, 6649 (2001).
166. L. Zhu, B. H. Calhoun, Q. Ge, R. P. Quirk, S. Z. D. Cheng, E. L. Thomas, B. S. Hsiao, F. Yeh, L. Liu, and B. Lotz, *Macromolecules* **34**, 1244 (2001).
167. L. Zhu, S. Z. D. Cheng, B. H. Calhoun, Q. Ge, R. P. Quirk, E. L. Thomas, B. S. Hsiao, F. Yeh, and B. Lotz, *Polymer* **42**, 5829 (2001).
168. E. A. DiMarzio, C. M. Guttman, and J. D. Hoffman, *Macromolecules* **13**, 1194 (1980).
169. M. D. Whitmore and J. Noolandi, *Macromolecules* **21**, 1482 (1988).
170. S. Nojima, S. Yamamoto, and T. Ashida, *Polym. J*. **27**, 673 (1995).
171. G. Reiter, G. Castelein, P. Hoerner, G. Riess, A. Blumen, and J.-U. Sommer, *Phys. Rev. Lett*. **83**, 3844 (1999).
172. G. Reiter, G. Castelein, P. Hoerner, G. Riess, J.-U. Sommer, and G. Floudas, *Euro. Phys. J. E* **2**, 319 (2000).
173. I. W. Hamley, M. L. Wallwork, D. A. Smith, J. P. A. Fairclough, A. J. Ryan, S.-M. Mai, Y.-W. Yang, and C. Booth, *Polymer* **39**, 3321 (1998).
174. J. P. A. Fairclough, S.-M. Mai, M. W. Matsen, W. Bras, L. Messe, S. Turner, A. J. Gleeson, C. Booth, I. W. Hamley, and A. J. Ryan, *J. Chem. Phys*. **114**, 5425 (2001).
175. D. R. Paul and S. Newman, Eds., *Polymer Blends* (Academic, London, 1978).
176. M. J. Folkes and P. S. Hope, Eds., *Polymeric Blends and Alloys* (Blackie, London, 1993).
177. S. Datta and D. J. Lohse, *Polymeric Compatibilizers: Uses and Benefits in Polymer Blends* (Hanser, Munich, 1996).
178. L. A. Utracki, *Commercial Polymer Blends* (Chapman and Hall, London, 1998).
179. H. Hasegawa and T. Hashimoto, in *Comprehensive Polymer Science. Second Supplement*, edited by S. L. Aggarwal and S. Russo (Pergamon, London, 1996), p. 497.
180. K. I. Winey, E. L. Thomas, and L. J. Fetters, *Macromolecules* **24**, 6182 (1991).
181. K. I. Winey, *Mater. Res. Soc. Symp. Proc*. **248**, 365 (1992).
182. K. I. Winey, E. L. Thomas, and E. L. Fetters, *Macromolecules* **25**, 2645 (1992).
183. M. W. Matsen, *Phys. Rev. Lett*. **74**, 4225 (1995).
184. C.-A. Dai, B. J. Dair, K. H. Dai, C. K. Ober, E. J. Kramer, C.-Y. Hui, and L. W. Jelinksi, *Phys. Rev. Lett*. **73**, 2472 (1994).
185. M. Sikka, N. N. Pellegrini, E. A. Schmitt, and K. I. Winey, *Macromolecules* **30**, 445 (1997).
186. M. D. Dadmun, *Macromolecules* **33**, 9122 (2000).
187. R. B. Thompson and M. W. Matsen, *Phys. Rev. Lett*. **85**, 670 (2000).
188. C. W. Macosko, P. Guégan, A. K. Khandpur, A. Nakayama, P. Marechal, and T. Inoue, *Macromolecules* **29**, 5590 (1996).
189. F. S. Bates, W. W. Maurer, P. M. Lipic, M. A. Hillmyer, K. Almdal, K. Mortensen, G. H. Fredrickson, and T. P. Lodge, *Phys. Rev. Lett*. **79**, 849 (1997).

190. M. A. Hillmyer, W. W. Maurer, T. P. Lodge, F. S. Bates, and K. Almdal, *J. Phys. Chem. B* **103**, 4814 (1999).
191. J. H. Lee, N. P. Balsara, R. Krishnamoorti, H. S. Jeon, and B. Hammouda, *Macromolecules* **34**, 6557 (2001).
192. F. S. Bates, W. Maurer, T. P. Lodge, M. F. Schulz, M. W. Matsen, K. Almdal, and K. Mortensen, *Phys. Rev. Lett*. **75**, 4429 (1995).
193. M. W. Matsen, *J. Chem. Phys*. **110**, 4658 (1999).
194. R. B. Thompson and M. W. Matsen, *J. Chem. Phys*. **112**, 6863 (2000).
195. K. Krishnan, K. Almdal, W. Burghardt, T. P. Lodge, and F. S. Bates, *Phys. Rev. Lett*. **87**, 098301 (2001).
196. T. L. Morkved, P. Stepanek, K. Krishnan, F. S. Bates, and T. P. Lodge, *J. Chem. Phys*. **114**, 7247 (2001).
197. T. Hashimoto, K. Yamasaki, S. Koizumi, and H. Hasegawa, *Macromolecules* **26**, 2895 (1993).
198. S. Koizumi, H. Hasegawa, and T. Hashimoto, *Macromolecules* **27**, 4371 (1994).
199. D. Yamaguchi, M. Takenaka, H. Hasegawa, and T. Hashimoto, *Macromolecules* **34**, 1707 (2001).
200. D. Yamaguchi and T. Hashimoto, *Macromolecules* **34**, 6495 (2001).
201. D. Yamaguchi, H. Hasegawa, and T. Hashimoto, *Macromolecules* **34**, 6506 (2001).
202. M. W. Matsen, *J. Chem. Phys*. **103**, 3268 (1995).
203. A. D. Vilesov, G. Floudas, T. Pakula, E. Y. Melenevskaya, T. M. Birshtein, and Y. V. Lyatskaya, *Macromol. Chem. Phys*. **195**, 2317 (1994).
204. A.-C. Shi and J. Noolandi, *Macromolecules* **28**, 3103 (1995).
205. M. W. Matsen and F. S. Bates, *Macromolecules* **28**, 7298 (1995).
206. H. Frielinghaus, N. Hermsdorf, K. Almdal, K. Mortensen, L. Messé, L. Corvazier, J. P. A. Fairclough, A. J. Ryan, P. D. Olmsted, and I. W. Hamley, *Europhys. Lett*. **53**, 680 (2001).
207. H. Frielinghaus, N. Hermsdorf, R. Sigel, K. Almdal, K. Mortensen, I. W. Hamley, L. Messé, L. Corvazier, A. J. Ryan, D. van Dusschoten, M. Wilhelm, *et al*., *Macromolecules* **34**, 4907 (2001).
208. P. D. Olmsted and I. W. Hamley, *Europhys. Lett*. **45**, 83 (1999).
209. J. Dlugosz, A. Keller, and E. Pedemonte, Kolloid Z.u.Z. *Polymere* **242**, 1125 (1970).
210. S. Collins, T. Mykhaylyk, and I. W. Hamley, unpublished work (2002).
211. G. Wanka, H. Hoffmann, and W. Ulbricht, *Macromolecules* **27**, 4145 (1994).
212. D. Zhao, J. Feng, Q. Huo, N. Melosh, G. H. Fredrickson, B. F. Chmelka, and G. D. Stucky, *Science* **279**, 548 (1998).
213. S. Koizumi, H. Hasegawa, and T. Hashimoto, *Macromolecules* **27**, 6532 (1994).